ACS APPLIED MATERIALS & INTERFACES

Research Article

www.acsami.org

The Effects of Ti Carbonization on the Nucleation and Oriented Growth of Diamond Films on Cemented Carbide

Xiang Yu,*[,†] Xi-an Zhao,[†] Ya-yun Liu,[†] Meng Hua,[‡] and Xin Jiang[§]

[†]School of Engineering and Technology, China University of Geosciences (Beijing), Beijing 100083, China

[‡]MBE Department, City University of Hong Kong, Hong Kong, China

[§]Institute of Materials Engineering, University of Siegen, Siegen 57076, Germany

ABSTRACT: To better understand the influence of carbonization of the Ti interlayer on diamond nucleation and growth, a series of Ti/diamond composite films were deposited on cemented carbide (WC:Co) substrates using a two-step deposition technique. The microstructural properties of the composite films were then characterized by scanning electron microscopy, X-ray diffractometry, and Raman spectroscopy, and their tribological properties were evaluated using a ball-on-disc tester and a metalloscope. The results showed that differences in carbonization for five Ti interlayers of different thicknesses led to variations in the preferred orientations of the TiC layers and in the subsequent nucleation and oriented growth of diamond. This suggests that Ti carbonization significantly influences the nucleation and growth of diamond and subsequently causes variations in the tribological properties of the produced diamond films.

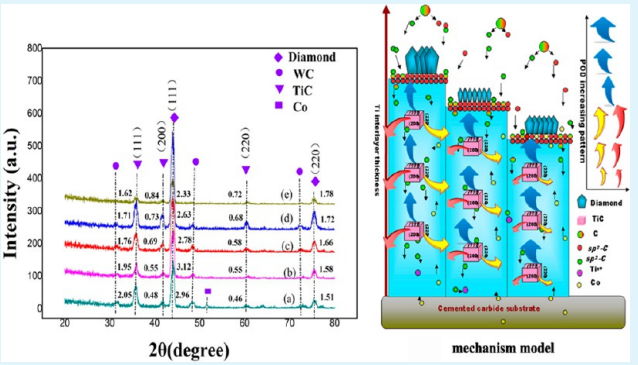

KEYWORDS: *diamond film, nucleation and growth mechanism, Ti carbonization, nucleation, oriented growth, tribological performance*

1. INTRODUCTION

Research has explored the relationship between the conditions of diamond film formation and the resulting film properties in order to produce materials with high hardness, a low friction coefficient, high thermal conductivity, and good chemical stability.[1] Because of these properties, diamond films are a very marketable material in fields such as mechanical engineering, electricity, optics, and tribology as well as for use in many other engineering structures. During diamond deposition, the conditions of the substrate/underlayer influence the adhesion and penetration characteristics of the C particles, which subsequently cause variations in the film properties. This is one of the main reasons preventing diamond-coated components from being more widely adopted in industry.[2]

Research on the substrate and on the nucleation and growth of diamond films has indicated that (i) the surface energy of a substrate affects the level and mobility of C atom migration, which subsequently changes the nucleation and grain size of the film being deposited,[3] and that (ii) the morphology and roughness of the deposited substrate surface influence the grain size and growth orientation of the diamond during the nucleation process.[4] However, little research has been performed on how the interactions between the deposited atoms and the substrate change the nucleation and growth of the diamond film by varying the energy and morphology of the substrate surface.

Geological exploration devices usually interact with geological elements such as slurry and rock, resulting in abrasive wear. The abrasive wear under such rough working conditions can be addressed by combining the hardest and wear-resistant diamond film with a cemented carbide (tungsten carbide: cobalt (WC:Co)) substrate. This combination has thus far proven to be one of the few applicable surface modification solutions. Cobalt in cemented carbide has a double-edged effect: (a) cobalt plays a role in binding WC particles together in the carbide structure, and hence, a higher Co content yields improved toughness of the carbide; and (b) the strong tendency of graphitization of cobalt during diamond deposition tends to restrict the nucleation of diamond during the initial growth period.

To develop diamond-coated carbide tools that combine the hardness of diamond with the toughness of carbide, studies are necessary to achieve such a combination prior to effectively deploying these hybrid tools. Approaches using materials that serve as "seedbeds" for diamond nucleation have recently been studied and implemented. Among these techniques, the use of metallic Ti as an interlayer material between the cemented carbide and the diamond film has generated significant interest.[5] The influence of metallic Ti on the diamond film is

Received: October 21, 2013
Accepted: March 13, 2014
Published: March 13, 2014

believed to be a result of (i) the metallic Ti reacting with the C and subsequently forming TiC within the interlayer during the deposition of the diamond film and (ii) the structure and the density of the carbonization-induced TiC varying with the surface conditions. Consequently, this tends to induce variations in the diamond nucleation density and behavior.[6] Such variations cause difficulties in fabricating diamond/Ti composite films with uniform properties. Furthermore, researchers are still unable to demonstrate how the properties of diamond vary when combined with carbonized Ti. This lack of knowledge on the effect of the state of the metallic Ti on the quality of the diamond/Ti composite film jeopardizes the implementation of this technology in many engineering applications.

Therefore, this study was initiated by depositing Ti interlayers with five different thicknesses on cemented carbide substrates using arc ion plating (AIP). Thereafter, diamond layers were deposited on top of each interlayered substrate by hot-filament activated chemical vapor deposition (HFCVD). We then proceeded to explore the mechanisms by which Ti carbonization affects diamond nucleation and growth. This exploration was mainly aimed at determining how Ti carbonization influences the growth orientation of the diamond film and its subsequent behavior.

2. EXPERIMENTAL DETAILS

The substrates in this study were all standard cemented carbide coupons of YG6 (WC-1.5 mm: Co-6%, sintered). Prior to deposition, the Co phase and oxides on the coupon surface were dissolved by dipping the coupons into an HNO_3 (50%) acid solution for 5 min. After this step, the following sequence was performed: (i) 5 min of ultrasonic cleaning in acetone to remove any surface contamination and (ii) rinsing in deionized water before drying with argon gas to prevent oxidation. Following cleaning, the substrates were individually coated with the Ti/diamond composite film using a two-step process consisting of (i) the use of AIP to deposit the Ti interlayer and (ii) the use of HFCVD to deposit the diamond layers on top of the interlayer. Table 1 lists the main deposition parameters for this process.

After the deposition process was completed, the surface and cross-sectional morphologies of the composite films were observed using scanning electron microscopy (SEM). The corresponding crystalline structures of the diamond and the individual Ti layers were analyzed and compared using X-ray diffractometry (XRD). Their degree of preferred orientation (POD) was subsequently determined from eq 1

$$[\mathrm{POD}]_k = \frac{\left(\frac{I_k}{I_s^k}\right)}{\sum_k^n \frac{1}{n}\left(\frac{I_k}{I_s^k}\right)} \quad (1)$$

where I_k is the measured relative intensity, I_s^k is the relative intensity in the same plane of the standard PDF card 32-1383, and n is the total number of reflection peaks obtained from the film. The bonding structures of the deposited films were investigated by Raman spectroscopy. The individual friction coefficients (COFs) were evaluated with a ball-on-disc tester under the following testing conditions: (i) film coupons attached to a disk slid against a Φ 4 mm Si_3N_4 ball, (ii) sliding velocity of 0.125 m/s, (iii) normal load of 5 N, (vi) humidity of 45 ± 2%, and (vii) temperature of 27 ± 2 °C. In addition, the coupon individual wear tracks were analyzed with a metalloscope.

Table 1. Deposition Parameters for the Two-Step Deposition Procedure for the Ti/Diamond Composite Films

AIP (first step for Ti layer disposition)		HFCVD (second step for diamond)	
parameters		parameters	
bias voltage (V)	200	CH_4/H_2 (vol %)	1
duty ratio (%)	50	flow rate (sccm)	400
rotating speed (HZ)	4	distance between filament and substrate (mm)	15
Arc current (A)	60	reaction pressure (kPa)	4
deposition pressure (Pa)	5×10^{-2}	deposition temperature (°C)	780
deposition temperature (°C)	200	filament temperature (°C)	1900
depositing speed (nm/min)	27	duration (min)	300
depositing time (min)	5, 10, 20, 30, 40	bias voltage (V)	−100
TiC layer thickness (nm)	152, 277, 594, 880,1067	diamond film thickness(μm)	10

3. RESULTS AND DISCUSSION

3.1. XRD Patterns. The XRD patterns of the five films with different specific Ti layer thicknesses are compared in Figure 1.

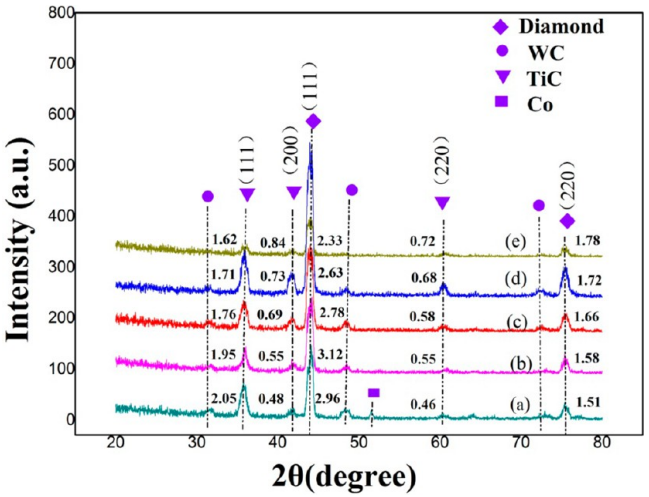

Figure 1. XRD patterns for the Ti/diamond composite films for different Ti deposition durations: (a) 5, (b) 10, (c) 20, (d) 30, and (e) 40 min. The numbers located beside the intense peaks are the PODs calculated using eq 1, specifically for indicating the orientation level of the individual peaks.

This comparison (Figure 1) allowed the identification of the following: (i) two diffraction peaks for the (111) and (220) diamond planes near the diffraction angles of 43.9° and 75.3° 2θ, respectively, and (ii) three peaks for the (111), (200), and (220) TiC planes around the diffraction angles of 35.9°, 41.7° and 60.5° 2θ, respectively. The absence of any signal for metallic Ti suggests the complete conversion of the metallic Ti to TiC within the Ti layers. This complete conversion may be the result of a phase transition from α-Ti to β-Ti because of the presence of high temperatures and exposure to H atoms during the diamond deposition process. Because carbon has a larger diffusion coefficient in β-Ti than in α-Ti,[7] the converted β-Ti may quickly react with the carbon atoms to form TiC at 700 °C. Except for the detection of a weak peak for cobalt at approximately 2θ = 51.52° for the 5-min-thick film (curve a in Figure 1), the lack of a Co signal suggests the achievement of a good buffer effect from the individual TiC layers.

dx.doi.org/10.1021/am404617m | ACS Appl. Mater. Interfaces 2014, 6, 4669−4677

The three PODs calculated with eq 1 (Figure 1) show that the TiC layer deposited over 5 min exhibited preferred growth orientation in the (111) plane. With the increase in the thickness of the Ti layer, the POD intensity shifted away from the (111) plane and subsequently moved to the other planes. This shift led to the growth of the TiC layer competitively occurring in the (111), (200), and (220) planes. Figure 1 indicates that the intensity of the diffraction peak for the $TiC_{(111)}$ lattice plane was considerably higher than those of the $TiC_{(200)}$ and $TiC_{(220)}$ planes, and the consistent occurrence of such a strong orientation of $TiC_{(111)}$ in all Ti layers implies that the preferentially oriented growth of TiC occurs in the (111) crystal face. This figure also illustrates the decrease in intensity of the diffraction peak for $TiC_{(111)}$ and the increase in those of $TiC_{(200)}$ and $TiC_{(220)}$ for greater Ti layer deposition times. The primary mechanisms behind this interesting phenomenon are believed to be a combination of the following items. The surface energy in the (111) growth plane is lower than those in the other counterpart planes, facilitating the growth of a face-centered cubic-structured film in that plane.[8] When the Ti interlayer is thin, a face-centered cubic TiC layer may rapidly form through the carbonization of the metallic Ti, such that the newly formed TiC has a preferred orientation in the (111) plane. Additionally, the formation of sp^2-C and sp^3-C from methane may occur during diamond deposition. The diffusion of these carbon forms into the Ti layer results in the formation of a dense amorphous phase in the Ti subsurface layer via a sub-plantation process. In such a process, the incorporation and assembly of the diffusing C species in the Ti subsurface layer tends to increase the stress in the amorphous layer, which induces the transformation of sp^2-C to sp^3-C. Meanwhile, the relaxation of and gradual decrease in the residual stress may also occur when (i) the C easily diffuses within the Ti layer and (ii) when the majority of the C species have successfully spread/diffused to the bottom of the Ti layer. Such phenomena have the tendency to reverse the sp^3-C bond back to a sp^2-C bond retroactively. When the thickness of the Ti layer increases, the carbon particles tend to diffuse deeper into the Ti layer and cause the formation and accumulation of more sp^2-C. This phenomenon may magnify the surface energy in the $TiC_{(111)}$ plane and reduce the surface energy in both the $TiC_{(200)}$ and $TiC_{(220)}$ planes,[9] resulting in a decrease in the POD of the $TiC_{(111)}$ plane and an increase in the PODs of the $TiC_{(200)}$ and $TiC_{(220)}$ planes.

Figure 1 also reveals that the preferred orientation degree (PODs) of diamond exhibits a decreasing tendency for $diamond_{(111)}$ and an increasing tendency for $diamond_{(220)}$ with an increase in the Ti layer thickness. This phenomenon may occur because changes in the orientations and structures of TiC induce corresponding changes in the diamond hetero-epitaxy grown thereon. This TiC sublayer may thus be considered a good candidate for diamond heteroepitaxy in a small lattice misfit to diamond. Upon increasing the Ti layer thickness, the pattern change of preferred orientations of the TiC crystals may respond to POD changes in the diamond crystal faces at (111) and (220).

An exceptional decrease can be observed for the peak intensities of TiC and diamond in curve e for the thickest Ti layer in Figure 1, relative to its four counterparts. This exceptional decrease implies that the Ti layer thickness favorable for the oriented growth of TiC and diamond has a critical range in this experiment. A layer such as that in Figure 1a, 5 min, is too thin to block Co contamination during diamond deposition. A layer such as that in Figure 1e, 40 min, may be too thick to induce a distinct decrease in the diffraction peaks. This intensity decrease may result from the competitive growth in the grains of TiC and subsequently of diamond, where the strong orientation tends to be weak (such as $TiC_{(111)}$ and $diamond_{(111)}$), and the weak one tends to be enhanced (such as $TiC_{(200)}$, $TiC_{(220)}$, and $diamond_{(220)}$).

3.2. Fracture and Surface Morphology. The cross-sectional microstructures of the deposited composite films are illustrated in Figure 2. A dense columnar structure was

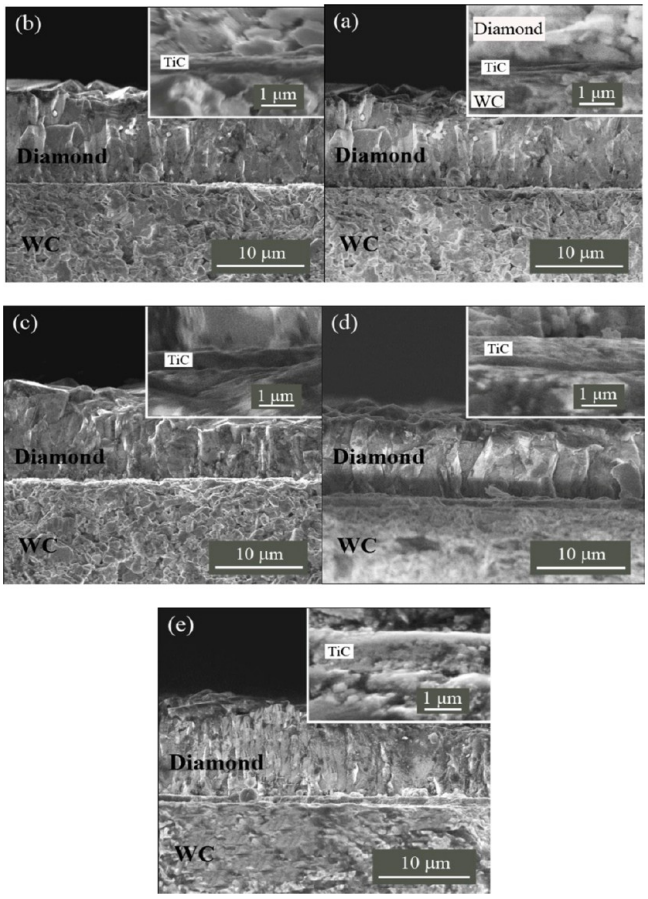

Figure 2. Cross-sectional morphologies of the composite films with layered structures containing the substrate/TiC interlayer (x in nm)/diamond: (a) x = 152, (b) x = 277, (c) x = 594, (d) x = 880, and (e) x = 1067.

observed growing perpendicular to the substrate surface for all the films. The thicknesses of the individual TiC layers, as shown in the insets of Figure 2, were measured to be approximately 152, 277, 594, 880, and 1067 nm, respectively. An analysis of these films provided an estimated average deposition rate for the Ti interlayer of 27 nm/min. Additionally, for a diamond layer thickness of approximately 10 μm, the average growth rate for the HFCVD diamond layer was approximately 2 μm/h. The surface morphologies of the Ti/diamond composite films suggested that the films were continuous and polycrystalline (see Figure 3). Many tiny ball-like diamond grains were also observed scattered around the grain boundaries. It is believed that these tiny-sized diamond crystallites were formed during diamond deposition second re-nucleation. Calculations using Image-Plus software showed that the average diamond grain sizes were approximately 4.37, 3.54,

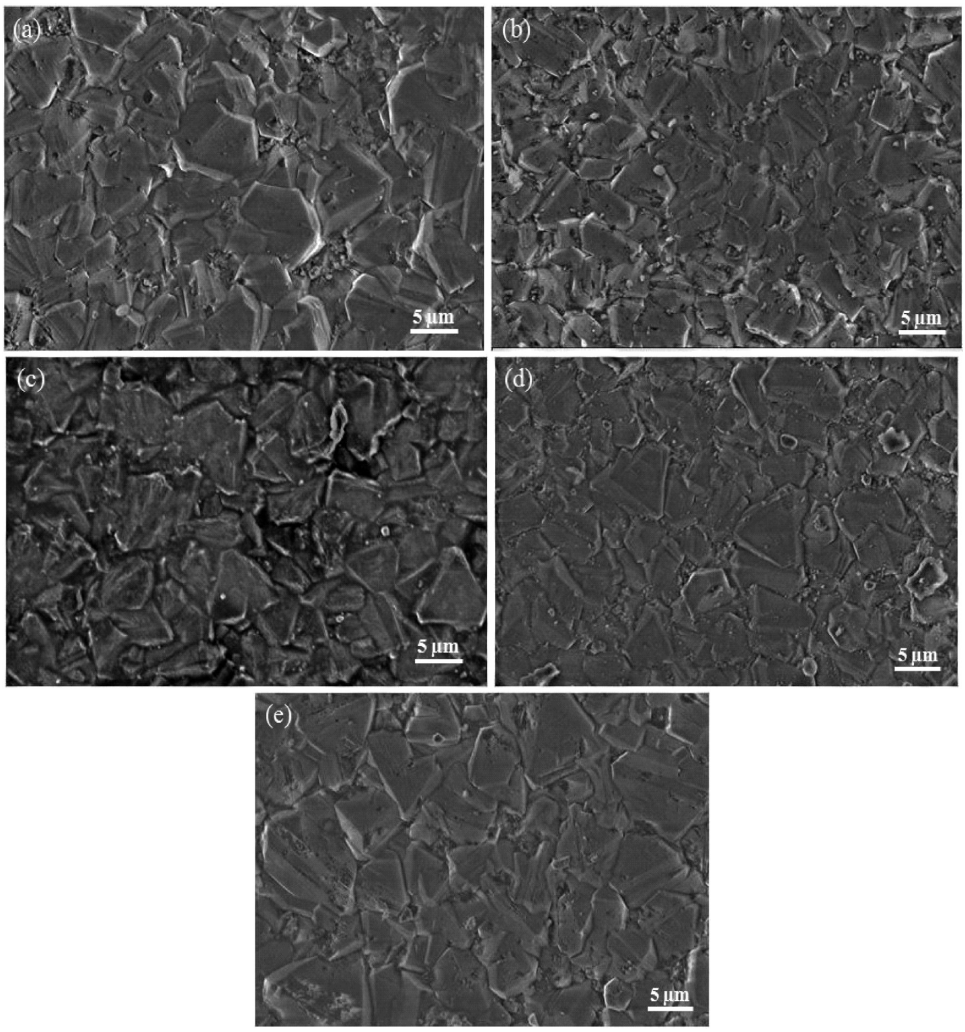

Figure 3. Surface morphologies of the diamond films for different Ti deposition duration times: (a) 5, (b) 10, (c) 20, (d) 30, and (e) 40 min.

4.42, 4.59, and 6.04 μm, respectively. This result indicates that the size increased with increasing TiC layer thickness.

This increasing tendency may be the result of the higher depletion of the C species by diffusion as the Ti layer thickens. Such depletion creates a larger variation in the TiC interlayer and causes the grain growth orientation to deviate from its normal path. These processes significantly impact the nucleation and growth of the diamond. The grain size of HFCVD diamond generally varies with the deposition process parameters, such as the temperature, pressure, and air supply, etc.[10] This study used constant deposition process parameters so that only the thickness of the TiC interlayer changed to investigate changes in the preferred growth orientation. The results suggest that the (111) plane in the TiC layer is a favorable path for the preferential growth of the diamond crystal nucleus because this plane has the lowest surface energy suitable for the assembly of C species in a small lattice misfit. This preferential growth orientation leads to a higher nucleation density of diamond, giving rise to smaller grain sizes. For the TiC interlayer with competitive growth oriented in the (111), (200), and (220) planes, the larger thicknesses resulted in longer complete cycle times for the diffusion reactions and the nucleation of the carbon atoms. Subsequently, these growth orientations yielded larger diamond crystal nuclei and grain sizes. When the (200) and (220) planes were enhanced in the TiC layer, the defect number within the TiC crystal changed. This type of defect subsequently induced changes in the internal stress and surface energy of the TiC layers. Consequently, the increase in the thickness of the TiC interlayer decreased the nucleation density and increased the grain size of the diamond. When the thickness of the TiC interlayer reached approximately 152 nm, an abnormal enlargement of the grain size in the composite film occurred because the Co phase from the substrate diffused to the interface and induced an increase in the surface energy at the interface through the formation of a graphite phase or an amorphous C phase. This tended to reduce the nucleation density of the film and coarsen the grains. When the Ti layer thickness reached 277 nm, the diamond grain size suddenly decreased because the infiltration of the Co atoms into the Ti layer was depleted. This depletion implies that the TiC interlayer became a favorable buffer for Co diffusion and diamond nucleation. Because the surface energy of the 277-nm-thick TiC layer in the (111) plane was the lowest, it was the preferential growth path, and diamond nucleation in this direction produced smaller diamond grains in the composite film.

3.3. Raman Spectra. Figure 4 shows the Raman spectra of the five diamond coatings. The spectra clearly demonstrate the presence of both diamond and graphite phases in the films. The

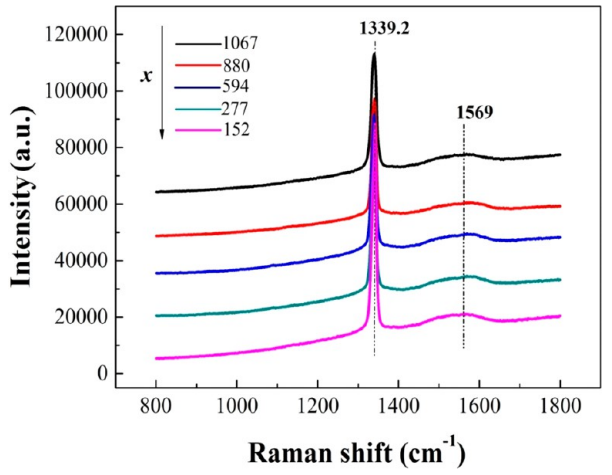

Figure 4. Raman spectra of the diamond films with TiC layers of different thicknesses.

characteristic peaks identified in the Raman spectra include the following: (i) an intense and narrow peak centered around 1340 cm^{-1}, indicating a high degree of sp^3-bonded diamond, and (ii) a broad peak between 1450 and 1620 cm^{-1} and centered at 1569 cm^{-1}, representing negligible sp^2-bonded carbon (graphite) and the induced stress variation in the C atoms within the films.[11] The fraction of sp^2 carbon was low and was estimated to be in the range of 1.4−2.1% of the total carbon content, increasing with thicker Ti layers.

The influence of the layer thickness on the Raman shifts of the Ti/diamond composite films is illustrated in Figure 5. The

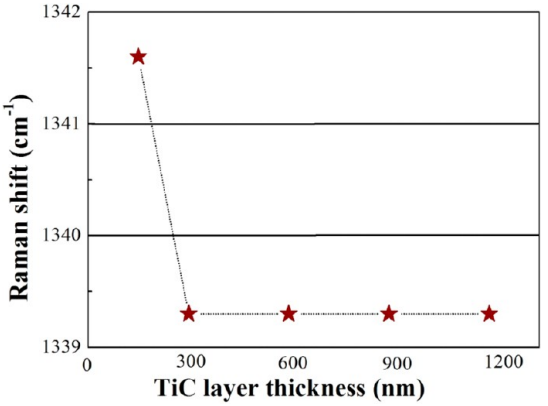

Figure 5. Influence of the layer thickness on the Raman shift of the Ti/diamond composite films.

Raman spectrum for the diamond composite film with a 152-nm-thick layer shifted as far as 1341.6 cm^{-1}, indicating the existence of residual compressive stress in the diamond coating. The residual stress calculated using the equation from ref 12 gives a value of σ_{Raman} = 3.312 GPa, for which the diamond Raman peak shift from the natural diamond line is 1332 cm^{-1}. When the deposition time was increased, the Raman spectra shifted to a lower frequency before stabilizing at 1339.2 cm^{-1}. Such high residual stress arises from the difference in the thermal expansion coefficients between the diamond coating and the depositing substrate.[13] Normally, the formation of a non-diamond phase for a diamond composite film with a 152-nm-thick interlayer is due to tge accumulation of inner-stress in the film caused by Co atom diffusion to the interface. The influence of the thickness of the TiC interlayer on the film peak position became insignificant after the TiC layer thickness reached a certain critical value.

3.4. Influence of the TiC Layer Thickness on the Friction Coefficient. The effect of the TiC layer thickness on the friction coefficients of the films is shown in Figure 6. The

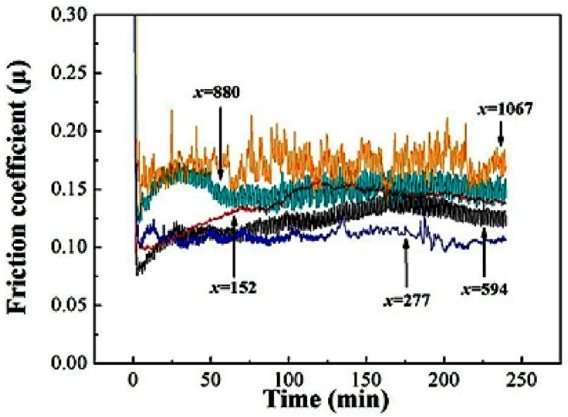

Figure 6. Friction coefficients of the as-deposited films for different deposition times when tested against a Si_3N_4 ball.

curves exhibit similar behavior and can be roughly categorized into three characteristic periods: an initial friction stage, a transitional period, and a steady-state phase. At the beginning of the friction test, the friction coefficients rapidly increased as a result of intense mechanical interactions between sharp diamond asperities and the counterpart surfaces. The friction coefficients on the diamond films in the steady-state phase appeared to increase as the TiC layer thickness increased. With an increase in the Ti layer thickness, the deposited diamond film exhibited a larger grain size, which may result in a rougher surface; in particular, the vibration observed during testing caused strong fluctuation in the x = 1067 nm curve. The friction coefficient of the deposited composite diamond films ranged from a minimum of approximately 0.09 for a layer thickness of 277 nm to a maximum of approximately 0.16 for a layer thickness of 1067 nm. The friction coefficients for the 152-, 594-, and 880-nm-thick layers were 0.13, 0.12, and 0.15, respectively.

3.5. Wear Track Morphology. The morphologies of a typical wear track on the five diamond films with differing TiC layer thicknesses are illustrated in Figure 7. The wear track for the diamond film with the 152-nm-thick layer (Figure 7a) was more severe than that for the diamond film with the 277-nm-thick layer (Fig. 7b). In general, the wear severity increased with the thickness of the TiC layers (cf., Figure 7b−e). Such severe wear damage may be because of changes in the diamond film performance as a consequence of variations in the crystalline structure and the physical properties of the TiC. Typically, the transformation of dense-hexagonal α-Ti to face-centered cubic β-Ti during the TiC formation process tends to increase the diffusion velocity of the carbon atoms (the rate of C diffusion in cubic β-Ti is 2×10^{-10} $m^2 \cdot s^{-1}$). Because β-Ti reacts more rapidly with C atoms than does α-Ti, loose, porous, face-centered cubic TiC forms.[14,15] Normally, the increases in the PODs for $TiC_{(200)}$ and $TiC_{(220)}$ can induce higher TiC hardness. However, the Vickers hardness (25 GPa) and Young's modulus (440 GPa) of the TiC were much lower than those of diamond. Therefore, the hardness of the diamond

dx.doi.org/10.1021/am404617m | ACS Appl. Mater. Interfaces 2014, 6, 4669−4677

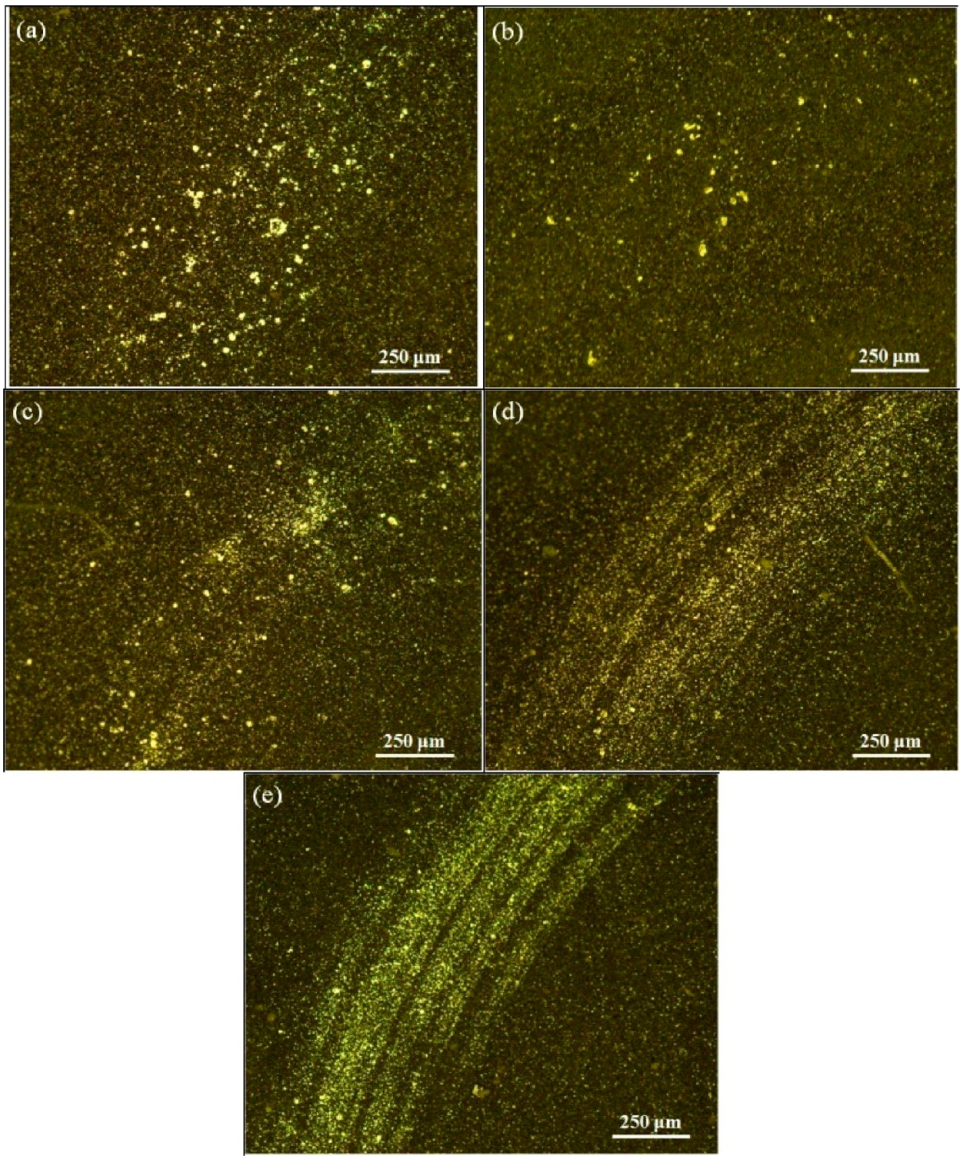

Figure 7. Wear tracks on the diamond films for different TiC layer thicknesses (x in nm): (a) x = 152, (b) x = 277, (c) x = 594, (d) x = 880, and (e) x = 1067.

composite films decreased as the thickness of the TiC layers increased.

As previously mentioned, the formation and increase in thickness of the loose, porous TiC layers usually results in a reduction in the wear- and scratch-resistance of the diamond composite film. Friction experiments indicated that the film surface was very susceptible to scratching and the formation of scratched scars. Increases in the Ti layer thickness generally facilitated the formation of large grains of diamond, which subsequently increased the roughness and the friction coefficient of the composite film.[16] Such roughening of the surface explains why the friction coefficient increased with the TiC layer thickness. The abnormal appearance of wear tracks (Figure 7a) on the composite film with a layer thickness of 152 nm may be attributed to the weaker interface binding energy and larger internal stress due to the formation of a non-diamond phase in the interface. Therefore, the nucleation density of diamond was reduced and the tribological properties of the composite film deteriorated.

3.6. Mechanism of Diamond Nucleation and Growth on Ti Interlayer. The results and discussion in sections 3.1−3.5 suggest that the grain growth and tribological performance of a diamond film can be altered by varying the thickness of the Ti interlayer. The carbonization process in the individual Ti layers has a significant effect on the preferred orientations of the TiC grains. This process will result in variations in diamond nucleation and oriented growth thereon. Figure 8 presents a model that is specifically proposed to illustrate the mechanism for diamond grain growth changes with varying thickness of the Ti interlayer.

The crystal nucleation of diamond results from a dynamic balance occurring at the Ti subsurface layer of diamond growth. This balance contains two competing and contradicting processes: (i) transformation of sp^3-C from sp^2-C within the Ti subsurface layer; and (ii) C species have significant mobility, allowing them to diffuse into the Ti interlayer. In process (i), the carbon in methane will be broken down to form various C species, such as sp^2-C and sp^3-C, during diamond deposition. These C species could penetrate into the Ti buffer layer via a

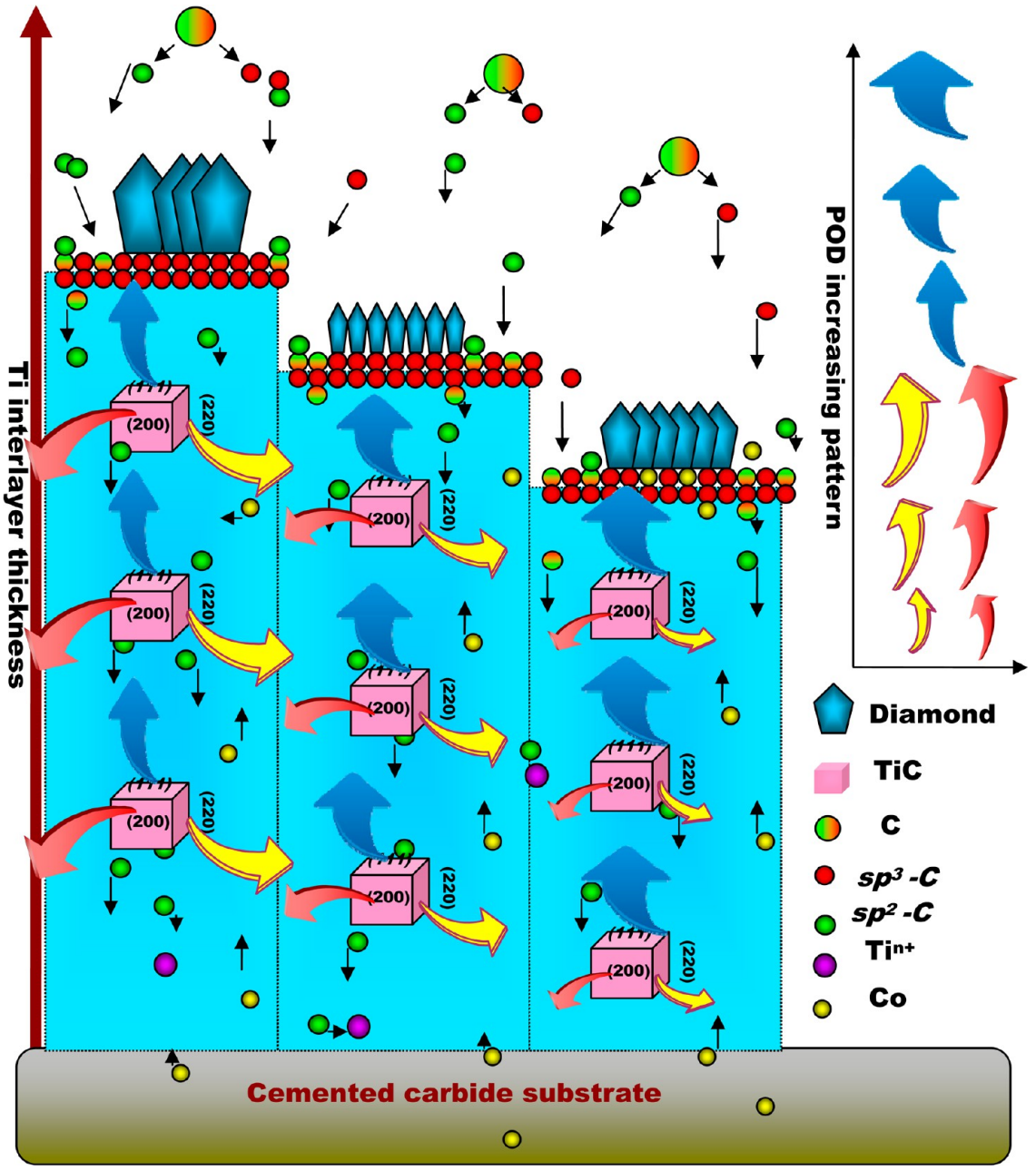

Figure 8. Mechanism for diamond grain growth changes as a function of Ti interlayer thickness. The three colored arrows (blue, red, and yellow) are the legends to illustrate the increasing patterns of PODs for the three TiC planes of (111), (200), and (220), respectively.

sub-plantation process and cause high compressive stress in the Ti subsurface layer. The sp^3-C can be generated in local areas of high compressive stress, and sp^2-C can be generated in local areas of low stress.[17] The increases in stress in the Ti subsurface layer lead to the transformation of the C species from sp^2-C to sp^3-C. For process (ii), the diffusion of the mobile C species tends to cause the stress to relax and to gradually decrease, which subsequently leads to the formation of sp^2-C from sp^3-C. The balance of these two processes (processes i and ii) results in the final condition of diamond nucleation.

The crystal orientation of TiC is closely related to that of the diamond grown thereon. Because the surface energy in the (111) growth plane is lower than those in the other counterpart planes, it facilitates the growth of a face-centered cubic-structured film in that plane. Because a face-centered cubic TiC layer may rapidly form through the carbonization of the metallic Ti, the newly formed TiC thus has a preferred orientation in the (111) plane. This subsequently formed TiC sublayer should be a good candidate for diamond heteroepitaxy in a small lattice misfit to diamond. Upon increasing the thickness of the Ti layer, the pattern change in the preferred orientations of the TiC crystals may result in the responsive oriented growth in the diamond faces of (111) and (220).

The Ti layer offers a special space for diamond nucleation and growth, and the influence of the Ti layer thickness on diamond growth and behavior must be considered. In a thin Ti layer, the diamond grains on the TiC layer grow along the (111) face and usually result in dense nucleation (Figure 1). However, the Ti layer is insufficient to buffer Co diffusion from the carbide substrate if it is too thin. This subsequently prompts

the formation of a non-diamond phase and increases the stress in the diamond layer (Figure 4). This stress rise jeopardizes diamond nucleation and leads to an abnormal decrease in the nucleation density and an increase in the grain size (Figure 3). The large diamond size roughens the film surface, which subsequently leads to an increased friction coefficient (Figure 6) and makes the film susceptible to wear failure (Figure 5). A TiC layer with a suitable thickness can normally block Co diffusion effectively and favor diamond nucleation and oriented growth; a typical example is curve b in Figure 1, whose PODs for the diamond faces (111) and (220) larger than those for curve a.

Further increases in the thickness cause competing growth of the TiC grains that are evident in the diamond crystals, causing the nucleation density of diamond to decrease and the film performance degrade. Increasing the thickness of the Ti layer leads to the need for a prolonged incubation period for the diamond nucleus and increase the amount of sp^2-C (Figure 8); with a thicker Ti layer, a significant amount of time is required for sp^2-C species to diffuse into the Ti layer and to reach the critical density necessaryfor diamond nucleation. Thus, the nucleation density of diamond will decrease with increasing nucleation time. Generally, a lower nucleation density results in large grain sizes.[18] The large grain sizes cause the diamond film to become coarser. Thus, we can observe in Figures 6 and 7 that with increases in the Ti layer thickness, the friction coefficient of the diamond film gradually increases, which yields a diamond film that is more vulnerable to wear.

In addition, the number of sp^2-C increases with increasing Ti layer thickness. A certain concentration of sp^2-C may increase the surface energy of the $TiC_{(111)}$ plane or decrease the surface energy of the $TiC_{(200)}$ and $TiC_{(200)}$ planes. Therefore, the preferred growth orientations of the three TiC planes change with increasing Ti layer thickness, which usually results in the three planes of TiC competing for crystal growth. This growth competition tends to change the PODs of the diamond faces, as observed in Figure 1, which shows a decrease in $diamond_{(111)}$ and an increase in $diamond_{(220)}$. Further growth competition may result in a sudden decrease in the grain number and size at the crystal faces, such as that shown in curve e in Figure 1.

In this manner, carbonization in Ti layers of different thicknesses affects the preferred orientations of the grains in the initial TiC and subsequently in the diamond grown thereon. Such Ti carbonization tends to change the nucleation density and the preferential growth orientation of the diamond and thus alters the tribological properties of the film. In this experiment, superior behavior belongs was observed in the filme with a 277-nm-thick Ti layer.

4. CONCLUSIONS

In this work, a series of Ti/diamond composite films were synthesized using a two-step technique involving the deposition of a Ti interlayer (examined with five different thicknesses in this work) on a cemented carbide substrate using AIP, followed by the deposition of diamond layers on the cemented carbide by HFCVD. The influence of carbonization on the microstructure and tribological properties of the composite films was also investigated. The results of the study are summarized as follows: (1) The carbonization of different thicknesses of Ti layers affected the grain growth orientation in the TiC layer. With increases in the Ti interlayer thickness, the amount of sp^2-C increased. Generally, an excess of active sp^2-C may increase the surface energy of the $TiC_{(111)}$ plane and decrease the surface energies of the $TiC_{(200)}$ and $TiC_{(220)}$ planes, leading to a change in the preferential growth orientation of the TiC layer from primarily in the (111) plane to primarily in the competing planes of (111), (200), and (220). This induces a POD decrease in the $diamond_{(111)}$ face and an increase in the $diamond_{(220)}$ face. (2) The variations in the preferential growth orientation of the TiC grains affected the grain size and nucleation density of the diamond film. The growth competition among the three planes in the TiC layer tended to vary the number of TiC crystal defects, the level of internal stress and the surface energy in the TiC layer, which is detrimental to diamond film nucleation. As the TiC thickness increased, the nucleation density decreased and the grain size of the diamond increased. (3) Both the grain size of diamond and the properties of the TiC layer affected the tribological performance of the composite film. During the diamond deposition process, the volume of the Ti layer increased due to the phase transition and the formation of a loose and porous TiC layer. The formation and increase in thickness of the loose, porous TiC layer led to a decrease in the wear and scratch resistance of the composite film. Moreover, the large grain size of the diamond tended to increase the surface roughness of the diamond film and increase the friction coefficient of the composite film. (4) The composite film with a 277-nm-thick TiC layer exhibited optimal tribological properties, which not only helped to prevent Co diffusion but also provided the lowest friction coefficient and the greatest wear resistance.

AUTHOR INFORMATION

Corresponding Author

*E-mail: yuxiang690625@aliyun.com. Phone: +86-10-82320255.

Notes

The reproducibility of the experiments and observations presented in the manuscript has been confirmed by independent batches. The AIP Ti layer was repeated by Beijing Powertech Co. Ltd., and the following HFCVD diamond layer was repeated by Langfang Supower Diamond Technology Co., Ltd. The two companies have confirmed that the deposition procedures and results are reproducible.

The authors declare no competing financial interest.

ACKNOWLEDGMENTS

This work was supported by (i) the National Natural Science Foundation of China under Grant No. 51071143, (ii) the Fundamental Research Funds for the Central Universities (2011YXL019, 2010ZY40, 2010ZY51), (iii) a Foundation of National Excellent Doctoral Dissertation of PR China under Grant FANEDD 201166 (specifically for the first author), and (iv) the National Professional Laboratory of Super-Deep Exploration.

REFERENCES

(1) Debabrata, P.; Lin, N. I. Grain-Size-Dependent Diamond-Nondiamond Composite Films: Characterization and Field-Emission Properties. *ACS Appl. Mater. Interfaces* **2009**, *7*, 1444−1450.

(2) Veillere, A.; Guillemet, T.; Xie, Z. Q.; Zuhlke, C. A.; Alexander, D. R.; Silvain, J.; Heintz, J.; Chandra, N.; Lu, Y. F. Influence of WC−Co Substrate Pretreatment on Diamond Film Deposition by Laser-Assisted Combustion Synthesis. *ACS Appl. Mater. Interfaces* **2011**, *3*, 1134−1139.

(3) Mylvaganam, K.; Zhang, L. C.; Xiao, K. Q. Origin of Friction in Films of Horizontally Oriented Carbon Nanotubes Sliding Against Diamond. *Carbon* **2009**, *47* (7), 1693−1700.
(4) Li, Y. S.; Tang, Y.; Yang, Q.; Maley, J.; Sammynaiken, R.; Regier, T.; Xiao, C.; Hirose, A. Ultrathin W−Al Dual Interlayer Approach to Depositing Smooth and Adherent Nanocrystalline Diamond Films on Stainless Steel. *ACS Appl. Mater. Interfaces* **2010**, *3*, 335−338.
(5) Barletta, M.; Rubino, G.; Valle, R.; Polini, R. Chemical Vapor Deposition of Highly Adherent Diamond Coatings onto Co-Cemented Tungsten Carbides Irradiated by High Power Diode Laser. *ACS Appl. Mater. Interfaces* **2012**, *4*, 694−701.
(6) Park, S.; An, J.; Potts, J. R.; Velamakanni, A.; Murali, S.; Ruoff, R. S. Hydrazine-Geduction of Graphite and Grapheme Oxide. *Carbon* **2011**, *49* (9), 3019−3023.
(7) Kumar, V.; Bergman, A. A.; Gorokhovsky, A. A.; Zaitsev, A. M. Formation of Carbon Nanofilms on Diamond for All-Carbon Based Temperature and Chemical Sensor Application. *Carbon* **2011**, *49* (4), 1385−1394.
(8) Kiran, V.; Sampath, S. Enhanced Raman Spectroscopy of Molecules Adsorbed on Carbon-Doped TiO_2 Obtained From Titanium Carbide: a Visible-Light-Assisted Renewable Substrate. *ACS Appl. Mater. Interfaces* **2012**, *4*, 3818−3828.
(9) Krivchenko, V. A.; Dvorkin, V. V.; Dzbanovsky, N. N.; Timofeyev, M. A.; Stepnaov, A. S.; Rakhimov, A. T. Evolution of Carbon Film Structure During Its Catalyst-Free Growth in the Plasma of Direct Current Glow Discharge. *Carbon* **2012**, *50* (4), 1477−1487.
(10) Dwivedi, N.; Kumar, S.; Malik, H. K. Nanostructured Titanium/Diamond-Like Carbon Multilayer Films: Deposition, Characterization, and Applications. *ACS Appl. Mater. Interfaces* **2011**, *3*, 4268−4278.
(11) Bo, Z.; Yu, K.; Lu, G.; Wang, P.; Mao, S.; Chen, J. Understanding Growth of Carbon Nanowalls at Atmospheric Pressure Using Normal Glow Discharge Plasma-Enhanced Chemical Vapor Deposition. *Carbon* **2011**, *49* (6), 1849−1858.
(12) Ferreira, N. G.; Abramof, E.; Corat, E. J.; Trava-airoldi, V. J. Residual Stresses and Crystalline Quality of Heavily Boron-Doped Diamond Films Analysed by Micro-Raman Spectroscopy and X-ray diffraction. *Carbon* **2003**, *41* (6), 1301−1308.
(13) Lu, P.; Gomez, H.; Xiao, X. C.; Lukitsch, M.; Durham, D.; Sachdeve, A.; Kumar, A.; Chou, K. Coating Thickness and Interlayer Effects on CVD-Diamond Film Adhesion to Cobalt-Cemented Tungsten Carbide. *Surf. Coat. Technol.* **2013**, *215*, 272−279.
(14) Li, C. M.; Wang, L. M.; Chen, L. X.; Liu, Z.; Hei, L. F.; Lu, F. X. Free-Standing Diamond Films Deposited by DC Arc Plasma Jet on Graphite Substrates with a Destroyable Ti Interlayer. *Diamond Relat. Mater.* **2009**, *18*, 1348−1352.
(15) Lee, S.T.; Lin, Z.D.; Jiang, X. CVD Diamond Films: Nucleation and Growth. *Mater. Sci. Eng.* **1999**, *25*, 123−154.
(16) Sarangi, S. K.; Chattopadhyay, A.; Chattopadhyay, A. K. Effect of Pretreatment, Seeding and Interlayer on Nucleation and Growth of HFCVD Diamond Films on Cemented Carbide Tools. *Int. J. Refract. Met. Hard Mater.* **2008**, *26*, 220−231.
(17) Lee, K. C.; Sprague, M. R.; Sussman, B. J.; Nunn, J.; Langford, N. K.; Jin, X. M. Entangling Macroscopic Diamonds at Room Temperature. *Science* **2011**, *334* (6060), 1253−1256.
(18) Konicek, A.R.; Grierson, D.S.; Sumant, A.V.; Friedmann, T.A.; Sullivan, J.P.; Gilbert, P. U. P. A. Influence of Surface Passivation on the Friction and Wear Behavior of Ultrananocrystalline Diamond and Tetrahedral Amorphous Carbon Thin Films. *Phys. Rev. Lett.* **2012**, *85* (15), 155448−155461.